Selectivity of Metallocene-Catalyzed Olefin Polymerization: A Combined Experimental and Quantum Mechanical Study. The *ansa*-$Me_2Si(Ind)_2Zr$ and *ansa*-$Me_2C(Cp)(Flu)Zr$ Systems

Manuela Borrelli, Vincenzo Busico,*,† Roberta Cipullo, and Sara Ronca

Dipartimento di Chimica, Università degli Studi di Napoli Federico II, Italy

Peter H. M. Budzelaar*,‡

Metal-Organic Chemistry, University of Nijmegen, The Netherlands

Received July 14, 2003; Revised Manuscript Received August 19, 2003

ABSTRACT: DFT calculations are reported for all possible insertions of ethene and propene in *rac*-$Me_2SiInd_2Zr{-}R]^+$ and $Me_2C(Cp)(Flu)Zr{-}R]^+$ (R = Et and *i*Pr). The results confirm the basic stereoregulation mechanism of Corradini. In addition, they provide an ordering of the possible sources of stereoerrors: chain misorientation is the main mechanism for unbranched (Et, *n*Pr) chains, whereas for the *β*-branched *i*Bu chain errors due to chain misorientation and chain−olefin syn orientation are equally likely.

Introduction

We recently reported in this journal[1] on a combined theoretical/experimental study of the *chemo*- and *regio*-selectivities of three nonchiral metallocene catalysts, namely $Cp_2Ti{-}R]^+$, $Cp_2Zr{-}R]^+$, and $Me_2SiCp_2Zr{-}R]^+$ (the latter modeled as $H_2SiCp_2Zr{-}R]^+$). Our aim was mainly to check how far, for these simple prototypical systems, a fully quantum-mechanical (QM) modeling of the active cation which does not explicitly include the solvent and the counterion is capable of reproducing the relative rates of all competing ethene and propene insertions in condensed phase. These relative rates were also measured specifically for this purpose with very high accuracy in order to provide a consistent and reliable reference data set. The fairly satisfactory agreement obtained is an indication that solvent and counterion effects, though undoubtedly important,[2] are rather indiscriminate for these catalysts, and also that olefin insertion is the rate-determining step on the reaction path (i.e., the insertion transition state is the highest point of the reaction path).

In the present paper, we extend our study to two well-known[3,4] *ansa*-zirconocene cations with chirotopic sites, i.e., *rac*-$Me_2SiInd_2Zr{-}R]^+$ and $Me_2C(Cp)(Flu)Zr{-}R]^+$ (Ind = 1-indenyl, Flu = 9-fluorenyl), for which *stereo*-selectivity becomes an additional, fundamental issue. The former species can be regarded as the ancestor of present-day C_2 symmetric metallocene catalysts for highly *isotactic* propene polymerization; the latter with its C_s symmetry opened the way to the synthesis of highly *syndiotactic* polypropylene. It is not surprising, therefore, that both have been addressed theoretically by a number of groups;[5] however, to the best of our knowledge, a fully quantum-mechanical study including all possible routes to *stereo*- and *regio*errors has never been reported. Here we present the results of such a study, and compare them with experimental ones, most of which were recently obtained in our laboratory by means of thorough ^{13}C NMR microstructural polymer analyses (see refs 4 and 6−8), as well as with those of part 1[1] for the simpler homologues $Cp_2Zr{-}R]^+$ and $Me_2SiCp_2Zr{-}R]^+$.

Computational Methods

All calculations were carried out with the Turbomole program[9] coupled to the PQS Baker optimizer.[10] Geometries were fully optimized as minima or transition states at the b3-lyp level[11] using the Turbomole SVP basisset on all atoms (def-SVP pseudopotential basis on Zr), and a fine ("m4") integration grid. To facilitate comparison with the Cp_2Zr and H_2SiCp_2Zr systems studied earlier using smaller basissets and partially constrained optimizations, these smaller systems were also fully reoptimized at the b3-lyp/SVP level (using Me_2SiCp_2Zr instead of H_2SiCp_2Zr). All stationary points were characterized by vibrational analyses; ZPE and thermal (enthalpy *and* entropy) corrections (1 bar, 273 K) from these analyses are included. All energies mentioned in text and tables are free energies. It should be noted that, although thermal corrections mostly improve agreement with experiment here, they also cause some "noise" in the results, presumably because very low-frequency modes cannot always be handled correctly.

The ethyl (Et) and isopropyl (*i*Pr) groups were used to simulate a primary and secondary growing polymer chain, respectively. For quantitative prediction of the enantioselectivity of propene insertion the Et residue is too small, so we have also checked enantioselectivity using *n*-propyl (*n*Pr) and isobutyl (*i*Bu) chain models.

For each cation we obviously examined only one of the two enantiomeric arrangements: the R,R ligand in *rac*-$Me_2SiInd_2Zr{-}R]^+$, and the *S* configuration of the Zr center in $Me_2C(Cp)(Flu)Zr{-}R]^+$.

Table S1 (see Supporting Information) contains total energies of all species studied. Rough estimates of combined solvation/counterion effects were made as described in ref 1. In brief, for each system, we assumed the following.

• $\{Mt(Et)(Ethene)]^+\}_{solv}$ is 6 kcal above $\{Mt(Et)]^+\}_{solv}$ + ethene. This estimate is based on calculations by Ziegler.[12] The *absolute* value is only important when one wants to make a comparison with experimental *activation energies* (which we do not attempt). The *relative* barriers considered here, instead, are *not* affected by this choice.

† E-mail: busico@chemistry.unina.it.
‡ E-mail: budz@sci.kun.nl.
* Corresponding author.

10.1021/ma034990v CCC: $25.00
Published on Web 09/24/2003

Table 1. Calculated Free Energies (kcal/mol, Relative to Zr−Et and Zr−*i*Pr Complexes) for Ethene and Propene Complexes and Insertion Transition States

system		Cp_2Zr		Me_2SiCp_2Zr		Me_2SiInd_2Zr			$Me_2C(Cp)(Flu)Zr$		
(E = ethene, P = propene)		gas phase	corr[a]	gas phase	corr[a]	enantioface[d]	gas phase	corr[a]	enantioface[d]	gas phase	corr[a]
$L_2Zr-Et]^+$	backskip TS	9.7		8.9			9.6			8.9	
	E complex	3.6	(6.0)	2.3	(6.0)		3.7	(6.0)		1.6	(6.0)
	E TS aw	9.8	12.3	7.8	11.5		10.3	12.6		8.8	13.2
	E TS tow						12.1	14.5		10.1	14.6
	P complex	3.3	6.7	−1.1	3.6		3.4	6.7		1.5	6.9
	P TS 1,2 anti aw[b]	13.7	17.2	11.4	16.1	*re*	13.9	17.3	*si*	12.5	18.0
	P TS 1,2 anti tow[b]					*si*	16.3	19.6	*re*	13.7	19.1
	P TS 1,2 syn aw[b]	17.1	20.5	14.3	19.0	*si*	17.4	20.7	*re*	14.9	20.3
	P TS 1,2 syn tow[b]					*re*	18.6	22.0	*si*	16.8	22.2
	P TS 2,1 anti aw[b]	17.8	21.2	15.2	19.9	*si*	18.0	21.3	*re*	19.7	25.1
	P TS 2,1 anti tow[b]					*re*	25.3	28.7	*si*	17.2	22.7
	P TS 2,1 syn aw[b]	18.5	22.0	15.8	20.5	*re*	23.4	26.7	*si*	16.4	21.8
	P TS 2,1 syn tow[b]					*si*	19.7	23.1	*re*	22.5	27.9
$L_2Zr-iPr]^+$	E complex	6.2	8.6	3.4	7.1		7.7	10.1		3.5	7.9
	E TS	10.2	12.6	8.5	12.1		12.4	14.7		11.4	15.8
	P complex	4.1	7.5	2.8	7.5		5.6	9.0		3.9	9.3
	P TS 1,2 aw[c]	16.9	20.3	15.1	19.8	*si*	19.4	22.8	*re*	17.4	22.8
	P TS 1,2 tow[c]					*re*	20.0	23.3	*si*	17.7	23.1
	P TS 2,1 aw[c]	18.4	21.8	16.0	20.6	*si*	20.6	24.0	*si*	18.2	23.7
	P TS 2,1 tow[c]					*re*	27.5	30.9	*re*	23.2	28.6

[a] Adjusted for solvation/counterion effects (see text). [b] aw = chain avoiding indenyl/fluorenyl ligand; tow = chain toward ligand. [c] aw = propene Me group avoiding indenyl/fluorenyl ligand; tow = propene Me group toward ligand. [d] Propene enantioface inserting at R,R-$Me_2SiInd_2Zr-R]^+$ or an S metal center of $Me_2C(Cp)(Flu)Zr-R]^+$.

•Solvation is the same for all isomeric olefin complexes and transition states.

•Adding a methyl group to either alkyl chain (e.g., Et → *i*Pr) or olefin (ethene → propene) decreases solvation by a "fudge factor" of 1 kcal/mol. This choice only affects the relative preference for ethene and propene insertion of each species, and the relative reactivities of different alkyl species. The value of 1 kcal/mol is admittedly somewhat arbitrary,[1] but we believe that assuming *no* steric effects would be even worse.

These assumptions allow us to put all reactions of a given alkyl cation on the same energy scale. From here on, we will always refer to the "corrected" values, unless indicated otherwise.

In all tables, we reported only the energies of the lowest-energy olefin complex structures, even where these do not directly correspond to the geometries for the insertion transition states. As discussed earlier, the olefin complexation energy does not affect the predicted product distribution anyway.[1]

Results and Discussion

General Considerations. With no exception, olefin insertion was found to proceed according to a standard Cossee mechanism,[13a,b] assisted by an α-agostic interaction of the migrating alkyl group at the transition state.[13c,d] Table 1 contains a compact presentation of all relevant QM results, including—for comparison—fully reoptimized data for the two achiral systems $Cp_2Zr-R]^+$ and $Me_2SiCp_2Zr-R]^+$ studied earlier. Table 2 compares regioselectivity for propene insertion in Et, *n*Pr, and *i*Bu chain models. Table 3 provides excerpts focusing on the calculated differences in insertion barriers determining the chemo-, enantio- and regioselectivities of all investigated $Me_2SiInd_2Zr-R]^+$ and $Me_2C(Cp)(Flu)Zr-R]^+$ species, and on their comparison with experimental ones where possible.

In the following, the conventional notations k_{xy} and $G^{\#}_{xy}$ are used to indicate the kinetic constant and activation free energy for monomer insertion "y" following insertion "x". The subscripts can be "E" for ethene; "p" ("primary") for 1,2-propene; and "s" ("secondary") for 2,1-propene. As an example, k_{ps} is the kinetic constant of 2,1-propene insertion in a growing chain with a 1,2-propene last-inserted unit. For insertion into a specific alkyl group, the abbreviation of this group appears as the first subscript: for instance, $k_{Et,p}$ and $G^{\#}_{Et,p}$ for 1,2-propene insertion into Zr−Et.

Table 2. Relative Barriers (kcal/mol) for Propene Insertion in $Me_2SiInd_2Zr-R]^+$ and $Me_2C(Cp)(Flu)Zr-R]^+$

system[a]		Me_2SiInd_2Zr		$Me_2C(Cp)(Flu)Zr$	
		enantioface[b]	$\Delta G^{\#}$	enantioface[b]	$\Delta G^{\#}$
$L_2Zr-Et]^+$	anti aw	*re*	(0)	*si*	(0)
	anti tow	*si*	2.4	*re*	1.1
	syn aw	*si*	3.5	*re*	2.3
$L_2Zr-nPr]^+$	anti aw	*re*	(0)	*si*	(0)
	anti tow	*si*	2.5	*re*	1.2
$L_2Zr-iBu]^+$	anti aw	*re*	(0)	*si*	(0)
	anti tow	*si*	4.1	*re*	3.0
	syn aw	*si*	3.2	*re*	2.4

[a] aw = chain avoiding indenyl/fluorenyl ligand; tow = chain toward ligand. [b] Propene enantioface inserting at R,R-$Me_2SiInd_2Zr-R]^+$ or an S metal center of $Me_2C(Cp)(Flu)Zr-R]^+$.

Olefin Binding. The calculated *free* energies of olefin complexation are nearly all positive, i.e., coordination is *endo*thermic, because of the large entropy of the gas-phase monomers (in the absence of thermal corrections, complexation is always downhill). From the *gas-phase* data in Table 1, one can see that ethene binds to $Me_2SiCp_2Zr-Et]^+$ more weakly than propene (by ca. 2 kcal/mol). This is no longer true for $Cp_2Zr-Et]^+$, $Me_2SiInd_2Zr-Et]^+$, and $Me_2C(Cp)(Flu)Zr-Et]^+$ (all ≈0 kcal/mol), mainly due to thermal corrections: propene is more constrained in these less open systems. Ethene coordinates more weakly to $Me_2SiInd_2Zr-Et]^+$ than to $Me_2SiCp_2Zr-Et]^+$ (also if thermal corrections are excluded). This may look somewhat surprising, since indenyl and fluorenyl ligands are usually considered to be weaker donors than cyclopentadienyls. Possibly, the polarizability of the arene rings has an effect that is more pronounced in the strongly electrophilic 12-*e* alkyl cations than in the 14-*e* alkyl−olefin complexes. Steric effects also play a role. For $Cp_2Zr-Et]^+$ and $Me_2SiCp_2Zr-Et]^+$, the most stable ethene complex is the *backside*

Table 3. Calculated Differences in Insertion Barriers (in kcal/mol) and Comparison with Experiment[4,6–8]

	$Me_2SiInd_2Zr-R]^+$			$Me_2C(Cp)(Flu)Zr-R]^+$		
	Et	*i*Bu	*i*Pr	Et	*i*Bu	*i*Pr
$\Delta G^{\#}_{R,p}$(enantio)	2.4 (obs >2)[a]	3.2 (obs 2.6)[b]	0.6 (obs 0.5)[c]	1.1 (obs 0.7)[d]	2.4 (obs 2.2)[e]	0.3
$\Delta G^{\#}$(regio) = $G^{\#}_{R,s} - G^{\#}_{R,p}$	4.0 (obs 3.2)[f]		1.2 (obs 1.8)[g]	3.9 (obs 3.9)[f]		0.9
$\Delta G^{\#}_{R,s}$(enantio)	5.4 (obs >3)[h]			3.2 (obs >3)[h]		

[a] $RT \ln k_{Ep(re)}/k_{Ep(si)}$. [b] $RT \ln k_{pp(re)}/k_{pp(si)}$. [c] $RT \ln k_{sp(re)}/k_{pp(si)}$. [d] $RT \ln k_{Ep(si)}/k_{Ep(re)}$. [e] $RT \ln k_{pp(si)}/k_{pp(re)}$. [f] $RT \ln k_{ps}/k_{pp}$. [g] $RT \ln k_{ss}/k_{sp}$. [h] $RT \ln k_{ps(si)}/k_{pp(re)}$.

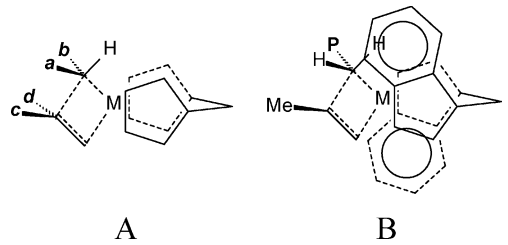

Figure 1. Chain and olefin orientations during insertion at a C_2-symmetric metallocene.

complex, where the olefin has approached from the direction opposite to the Zr−H β−agostic interaction. For the more hindered $Me_2SiInd_2Zr-Et]^+$ and $Me_2C(Cp)(Flu)Zr-Et]^+$ systems, this arrangement causes repulsion between the olefin and an arene ring of the ligand. Instead, the most stable complexes have structures without β-agostic interaction, which allows the coordinated olefin to move to the front of the complex and avoid repulsive interactions with the arene ring.

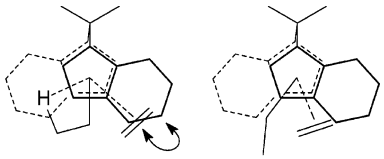

Propene Insertion. 1. Enantioselectivity. *rac*-$Me_2SiInd_2Zr-R]^+$ and $Me_2C(Cp)(Flu)Zr-R]^+$ species are known[3,4] to promote *isotactic* and *syndiotactic* propene polymerization, respectively, via 1,2-monomer insertion. Regioselectivity will be discussed in a subsequent section; here we focus on the factors determining enantioselectivity.

The widely accepted mechanism of stereocontrol for *rac*-$Me_2SiInd_2Zr-R]^+$ based on the so-called "growing chain orientation effect", originally introduced by Corradini on the grounds of molecular mechanics (MM),[14] and supported by later QM/MM studies of Morokuma[15,16] and Moscardi,[17] assumes that

- For a generic bis(Cp) metallocene, the four-center transition state for olefin insertion looks like Figure 1A, where the growing chain can point either "up" (position ***a***) or "down" (position ***b***).
- Substituents, when present, may favor either chain position ***a*** or ***b***. In particular, in a C_2-symmetric *ansa*-bis(indenyl) system (Figure 1B), the chain avoids the arene rings of the indenyl groups.
- The methyl group of the incoming monomer, in turn, avoids the chain, i.e., prefers an anti orientation: ***d*** if the chain is in position ***a***, or ***c*** if the chain is in position ***b***.

The model can easily be extended to $Me_2C(Cp)(Flu)Zr-R]^+$ systems. Figure 1B, indeed, is locally representative of the favored transition state at each of the two *enantiotopic* sites, and the *syndiotactic* selectivity is the natural result of the regular alternation of monomer insertion at these sites after chain-migratory insertion. In contrast with C_2-symmetric species with *homotopic* sites, chain "back-skip" (movement of the growing chain from one metal site to the other) can also introduce stereo-errors here. Therefore, for C_s-symmetric catalysts the *enantio*selectivity represents an upper limit of the *stereo*selectivity, which can be approached under conditions of negligible chain back-skip (i.e., high monomer concentration, low polymerization temperature).[3,4]

Our calculations (Table 1) basically agree with the Corradini model, and confirm the interplay of chain and monomer orientation. In particular, they are as follows.

Preferred Chain Orientation Relative to the Ligand. At each given cation, the preference for a specific chain orientation can already be seen in the Et/ethene insertion, where the transition state (TS) with the ethyl group toward (tow) the indenyl or fluorenyl arene ring is about 1.5 kcal/mol less favorable than the one with the chain pointing away (aw) from the ligand. For a prochiral monomer like propene, of course, this preference becomes enantio-discriminating.

For $Me_2SiInd_2Zr-Et]^+$:

$$G_{Et,p}{}^{\#}(\text{anti tow}) - G_{Et,p}{}^{\#}(\text{anti aw}) = G_{Et,p}{}^{\#}(si \text{ tow}) - G_{Et,p}{}^{\#}(re \text{ aw}) = 2.6 \text{ kcal/mol}$$

For $Me_2C(Cp)(Flu)Zr-Et]^+$:

$$G_{Et,p}{}^{\#}(\text{anti tow}) - G_{Et,p}{}^{\#}(\text{anti aw}) = G_{Et,p}{}^{\#}(re \text{ tow}) - G_{Et,p}{}^{\#}(si \text{ aw}) = 1.2 \text{ kcal/mol}$$

Not unexpectedly, the difference is larger when R is *i*Bu: 4.1 kcal/mol for Me_2SiInd_2Zr and 3.0 kcal/mol for $Me_2C(Cp)(Flu)Zr$.

Orientation of the Propene Methyl Group Relative to the Chain. In our earlier study on achiral metallocenes,[1] we found that insertions with the propene methyl group anti to the chain are 3−4 kcal/mol more favorable than syn orientations. We see the same effect here (Table 2, R/propene 1,2 anti aw vs 1,2 syn aw): for Me_2SiInd_2Zr, 3.5 kcal/mol when R = Et, 3.2 kcal/mol when R = *i*Bu; for $Me_2C(Cp)(Flu)Zr$, 2.3 kcal/mol when R = Et, 2.4 kcal/mol when R = *i*Bu.

Thus, the two parts of the Corradini model are indeed reproduced. In addition, the data in Table 1 make it possible to compare the two possible sources of misinsertions, i.e., chain or propene misorientation. According to earlier MM studies,[14] chain misorientation (propene anti to chain tow) would be dominant. From our calculations, this appears to be true for insertion into Zr−Et, where propene misorientation (propene syn to chain aw) "costs" more (by ca. 2 kcal/mol) and also for Zr−*n*Pr. On the other hand, for insertion into Zr−*i*Bu, which is more representative of a growing polypropylene chain, we find that the two paths are practically equivalent (see Figures 2 and 3). This seems to be due

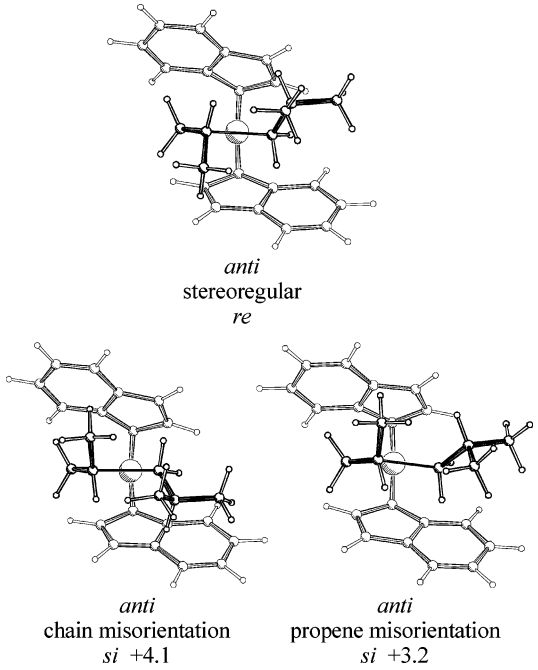

Figure 2. Transition states and relative barriers (kcal/mol) for regular and irregular 1,2-propene insertion in $Me_2SiInd_2Zr{-}i\mathrm{Bu}]^+$. Projection is along Zr−Si; the Si-bound Me groups have been omitted for clarity.

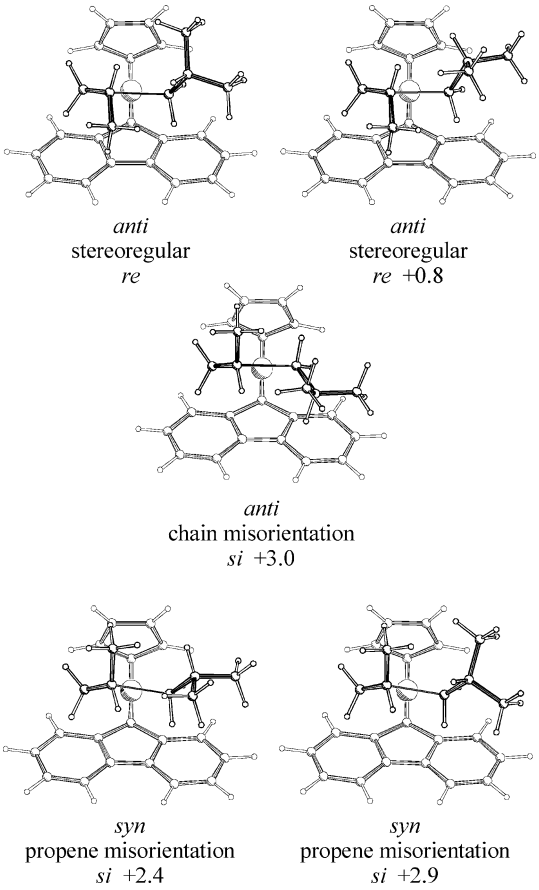

Figure 3. Transition states and relative barriers (kcal/mol) for regular and irregular 1,2-propene insertion in $Me_2C(Cp)(Flu)Zr{-}i\mathrm{Bu}]^+$. Projection is along $Zr{-}C(Me_2)$; the isopropylidene Me groups have been omitted for clarity. Absolute configurations are shown inverted for easy comparison with Figure 2.

to the syn transition states taking up less space in the mouth of the complex, which is more significant for β-branched alkyl chains than for *n*-alkyl chains. The figures also show that in the transition states for syn insertion, the four-membered ZrCCC ring is much more puckered than in the anti transition states.

For the $Me_2SiInd_2Zr{-}i\mathrm{Bu}]^+$ model system, we find only one low-lying transition state each for the three paths of stereoregular, anti-irregular, and syn-irregular insertion. For $Me_2C(Cp)(Flu)Zr{-}i\mathrm{Bu}]^+$, however, we find *two* low-lying transition states each for the regular and syn-irregular paths, which differ only in the orientation of the *i*Bu chain.

Let us comment now on the match with experiment (Table 3). From ^{13}C NMR polypropylene configuration analysis, we measured a difference in activation free energy between 1,2-propene insertion with the two enantiofaces in homopolymerization of $\Delta G^{\#}_{pp}$(enantio) = 2.6 kcal/mol for *rac*-$Me_2SiInd_2ZrCl_2$/MAO,[18] 2.2 kcal/mol for $Ph_2C(Cp)(Flu)ZrCl_2$/MAO[19] (MAO = methylalumoxane). This should be contrasted with the calculated values of 3.2 and 2.4 kcal/mol, respectively. The calculated value for *rac*-$Me_2SiInd_2ZrCl_2$/MAO is too high, but the lower enantioselectivity of $Me_2C(Cp)(Flu)ZrCl_2$/MAO is correctly reproduced.

The partial loss of enantioselectivity predicted for 1,2-insertion into Zr−Et, particularly for the sterically more open $Me_2C(Cp)(Flu)Zr$ system ($\Delta G^{\#}_{Et,p}$(enantio) = 1.1 kcal/mol), is also in line with experimental observations; indeed, in propene/ethene copolymerization promoted by $Ph_2C(Cp)(Flu)ZrCl_2$/MAO, we found a $\Delta G_{Ep}{}^{\#}$(enantio) = 0.7 kcal/mol.[8]

For C_s-symmetric catalysts like $Me_2C(Cp)(Flu)Zr{-}R]^+$, we have already noted that chain back-skip can be an additional source of stereoerrors. These are readily identified by ^{13}C NMR in the polymers, because they are of ...*rrrrmrrr*... type, whereas those formed by faults of enantioselection are of ...*rrrmmrrr*... type.[3,4] In the case of catalysts with homotopic sites (like *rac*-$Me_2SiInd_2Zr{-}R]^+$), this process has obviously no effect on the stereochemistry.

The number of theoretical studies dealing with back-skip is rather limited. Guerra looked at the relative stabilities of preinsertion intermediates using MM techniques.[20] Bierwagen[21] compared a number of different metals for back-skip in Cp_2MMe species, and concluded that the potential-energy curve for movement of the methyl group between the two positions is generally rather flat, leading to easy back-skip. However, this conclusion needs not be valid for higher alkyls for the follwoing reasons:

- Higher alkyl groups have a β-agostic interaction which must be broken for back-skip to occur.
- The alkyl must rotate around the M−C bond, which requires considerable space near the metal atom. Hence, rotation may have to occur at the most open position of the metallocene wedge, even if this is not the preferred chain position.

Indeed, Jensen reported that for $H_2CCp_2Zr{-}Pr]^+$, back-skip is a multistep process:[22] first the β-agostic interaction is broken and the chain switches to an α-agostic orientation, and then in the rate-determining step the chain switches the agostic interaction to the other α-hydrogen while passing through the "planar" arrangement around Zr.

Our calculations produce back-skip barriers of ca. 9−10 kcal/mol for all $L_2Zr{-}Et]^+$ systems studied, and also for $Cp_2Ti\text{-}Et]^+$ (not included in Table 1) and $L_2Zr{-}n\mathrm{Pr}]^+$ and $L_2Zr{-}i\mathrm{Bu}]^+$. In agreement with Jensen,[22] we

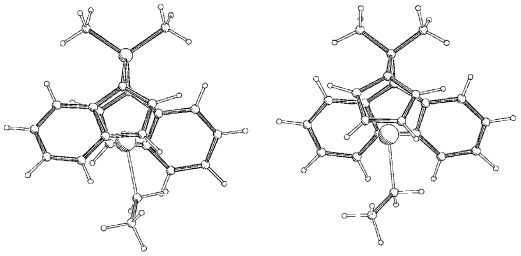

A B

Figure 4. Calculated transition states for back-skip in (A) $Me_2SiInd_2Zr-Et]^+$ and (B) $Me_2C(Cp)(Flu)Zr-Et]^+$.

conclude that back-skip barriers for higher alkyls can be substantially larger than for methyls. In contrast to the results obtained by Bierwagen, we do not find a strong dependence of the barrier on either the nature of the metal or the bending angle of the metallocene; this reinforces the idea that the two factors mentioned above are much more important to the back-skip barrier than the "intrinsic" barrier as calculated for methyl complexes. Figure 4 shows the calculated transition states for back-skip in $Me_2SiInd_2Zr-Et]^+$ and $Me_2C(Cp)(Flu)Zr-Et]^+$.

It is not easy to put the calculated barriers on the same scale as the insertion ones, since the crude solvent correction we employ (which does not affect the relative olefin insertion barriers) enters directly here; therefore, we do not attempt comparisons with experimental values.

Propene Insertion. 2. Regioselectivity. The calculated regioselectivity of propene insertion into Zr−Et is rather similar for all systems studied (chiral and achiral), with a preference $\Delta G^{\#}$(regio) of ca. 4 kcal/mol in favor of the 1,2 (primary) mode. For the two chiral zirconocenes, in particular, the agreement with experiment[6,7] (Table 3) is within the error limits of the theoretical approach.

From Table 1 it can be seen that, for Me_2SiInd_2Zr, 2,1-insertion into Zr−Et is enantioselective in favor of the enantioface *opposite* to that preferred in 1,2-insertion; the latter indeed brings the methyl group in *direct* steric contact with one of the two indenyl ligands (a much more unfavorable interaction than the *indirect*, chain-mediated one governing 1,2-insertion stereochemistry). This is in full agreement with the experimental finding (Table 3).[3,4]

A fairly high enantioselectivity of 2,1-insertion is predicted also at each of the two enantiotopic sites of $Me_2C(Cp)(Flu)Zr$, although this time the preferred enantioface would be the *same* favored in 1,2-insertion. This is seemingly in conflict with experimental observations suggesting that 2,1-insertion for $Ph_2C(Cp)(Flu)ZrCl_2$/MAO is substantially stereoirregular.[8] However, one should recall that—as seen before—a secondary insertion is ca. 1000 times slower than a primary one (Table 3), which implies that, relative to it, the conditional probability of a competing event of chain back-skip is 1000 times higher. Even in bulk monomer, this is enough to "scramble" the chain between the two sites prior to 2,1-insertion, which results in a lack of *stereo*selectivity (but *not* of *enantio*selectivity).

We note that, in the earlier literature, the regioregularity of syndiotactic polypropylene produced with C_s-symmetric *ansa*-zirconocenes had been overestimated, both in absolute sense and relative to that of isotactic polypropylene made with C_2-symmetric *ansa*-metallocenes, due to an inadequate signal-to-noise ratio in the ^{13}C NMR characterizations.[4,7] To explain the apparent high regioregularity, Guerra proposed a rather elaborate kinetic model in which catalyst regioselectivity would stem from the enantioselectivity of the competing 1,2- and 2,1-insertions and the possibility of olefin rotation in the coordination sphere of the metal.[23] In light of our experimental and theoretical results, such a model seems unnecessary.

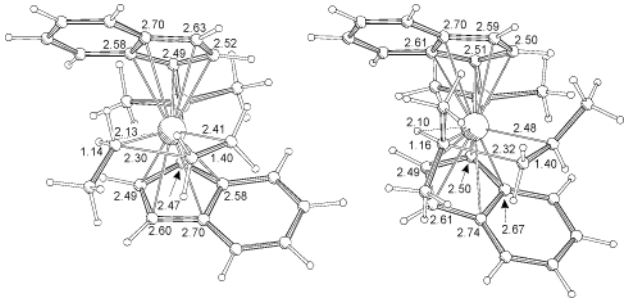

Figure 5. Calculated transition state geometries (bond lengths in Å) for insertion of ethene in Zr−Et and 2,1-insertion of propene in Zr−*i*Pr in the Me_2SiInd_2Zr system. The structures are drawn with the top indenyl ring in the same orientation. Numbers at the indenyl carbons are distances to the Zr center.

After a 2,1-insertion, the resulting secondary alkyl has a higher barrier toward further propene insertion by about 4 kcal/mol. Table 3 shows that, for insertion into Zr−*i*Pr, the 1,2 mode is still the preferred one, although with a much lower selectivity than at Zr−Et ($\Delta G^{\#}$(regio) of ca. 1 kcal/mol instead of 4). The insertion, moreover, is predicted to be practically nonenantioselective ($\Delta G^{\#}_{iPr,p}$(enantio) = 0.6 for Me_2SiInd_2Zr, 0.3 kcal/mol for $Me_2C(Cp)(Flu)Zr$). All this is in complete agreement with experiment (Table 3).

Ethene vs Propene Insertion. Chemoselectivity. From Table 1, one can see that ethene insertion into Zr−Et (which closely mimics the propagation step in ethene homopolymerization) occurs with similar barriers for all four zirconocenes. The competition between ethene and propene insertion in the same bond is also similar, the latter always being more difficult by 3−5 kcal/mol. Once again, we may say that this is in line with experiment, but with a tendency of the calculations to overestimate the difference in reactivity of the two monomers. For both *rac*-$Me_2SiInd_2ZrCl_2$/MAO and $Me_2C(Cp)(Flu)ZrCl_2$/MAO, the experimental value of the reactivity ratio $r_E = k_{EE}/k_{EP}$ is on the order of 10−20.[24,25]

Ligand Flexibility during Insertion. Compared to cyclopentadienyl, indenyl and fluorenyl ligands have an increased tendency to change their hapticity, e.g., via (partial) $\eta^5 \rightarrow \eta^3$ slippage. We can clearly see this happening in some of our structures. For example, Figure 5 compares the ligand−Zr arrangement of the crowded transition state for 2,1-insertion of propene in Zr−*i*Pr with the less crowded transition state for ethene insertion in Zr−Et. The increased flexibility of the Me_2SiInd_2Zr system over the Me_2SiCp_2Zr system is obvious from the larger bond length changes (up to 0.09 Å) in the former system. Figure 6 shows that for the same reactions of the $Me_2C(Cp)(Flu)Zr$ system, significant bond length changes occur at the fluorenyl part of the ligand but *not* at the Cp part. This, together with the variability at the transition state of Zr−C and C−C bond lengths we reported earlier for the Cp_2Zr and H_2SiCp_2Zr systems, illustrates that one should be very careful

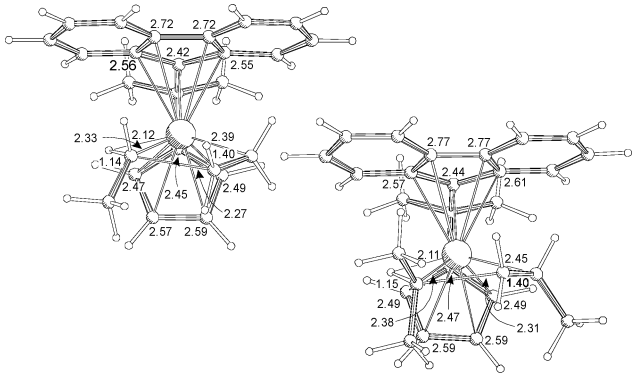

Figure 6. Calculated transition state geometries (bond lengths in Å) for insertion of ethene in Zr−Et and 2,1-insertion of propene in Zr−*i*Pr in the $Me_2C(Cp)(Flu)Zr$ system. The structures are drawn with the fluorenyl ring in the same orientation. Numbers at the fluorenyl carbons are distances to the Zr center.

in making assumptions about transition state geometries for use in, e.g., MM calculations.

Conclusions

In a previous paper,[1] we showed that full-QM calculations are able to reproduce to a fairly satisfactory extent the experimental chemo- and regioselectivities in ethene and propene (co-)polymerization of prototypical bridged and unbridged *achiral* metallocene cations, even without taking the counterion and the solvent explicitly into account. In the present one, we now demonstrate that the same holds for two well-known[3,4] *ansa*-zirconocene systems with chirotopic sites, namely *rac*-$Me_2SiInd_2Zr-R]^+$ and $Me_2C(Cp)(Flu)Zr-R]^+$, for which the enantioselectivity in propene insertion becomes an additional, fundamental issue.

In the latter respect, in particular, the calculations confirmed the well-known Corradini "growing chain orientation mechanism" of stereoregulation,[6] and provided an ordering for the various sources of stereoerrors as a function of the alkyl group bound to the metal: for R = Et, we found that chain misorientation is dominant, whereas chain and monomer misorientation contribute similarly for the larger *i*Bu group, which should be more representative of a real polymer chain.

Concerning the regioselectivity, the preference for 1,2- over 2,1-insertion was correctly reproduced. Complete agreement with the experiment was also achieved on the tendency of the occasional 2,1 units to remain isolated. For Me_2SiInd_2Zr, the experimentally observed very high preference of the latter to occur with the enantioface opposite to that favored for 1,2-insertion and the lower enantioselectivity of the 1,2-insertion immediately following a regiodefect were also reproduced.

Despite the remarkably good overall match between experimental and calculated data, it is important to realize that, at the present level of calculation and with the admittedly crude approximations of solvent and counterion effects, the uncertainty in the calculated values even of *relative* insertion barriers is expected to be at least 1 kcal/mol. Therefore, estimates of selectivity, which require to compare the barriers of two competing processes, can differ by up to 2 orders of magnitude from the experimental values and are still to be considered "in agreement" with them. In our opinion, this is not yet good enough to "predict" (in literal sense) catalyst behavior; however, it definitely allows ex post rationalization, and should already represent a valid tool for rational improvement of existing catalysts.

Acknowledgment. V.B. and R.C. acknowledge the Italian Ministry for University (PRIN 2002) and P. B. Sabic EPC and the Dutch Polymer Institute (Project #104), for financial assistance. The NMR characterization of all polymers was carried out at the "Centro di Metodologie Chimico-Fisiche" of the University of Naples "Federico II".

Supporting Information Available: Table S1, containing total energies and thermal corrections for all molecules studied (2 pages). This material is available free of charge via the Internet at http://pubs.acs.org. Optimized geometrical parameters for all species are available on request from P.B.

References and Notes

(1) Borrelli, M.; Busico, V.; Cipullo, R.; Ronca, S.; Budzelaar, P. H. M. *Macromolecules* **2002**, *35*, 2835.

(2) See, e.g.: Lanza, G.; Fragala, I. L.; Marks, T. J. *Organometallics* **2002**, *21*, 5594 and references cited there.

(3) Reviews: (a) Coates, G. W. *Chem. Rev.* **2000**, *100*, 1223. (b) Resconi, L.; Cavallo, L.; Fait, A.; Piemontesi, F. *Chem. Rev.* **2000**, *100*, 1253.

(4) (a) Review: Busico, V.; Cipullo, R. *Prog. Polym. Sci.* **2001**, *26*, 443. (b) Backside attack would have the same effect as back-skip followed by frontside attack. However, the calculated barrier for backside attack, 4.2 kcal/mol higher than frontside attack already for the Cp_2Zr system with an ethyl chain (Lohrenz, J. C. W.; Woo, T. K.; Fan, L.; Ziegler, T. *J. Organomet. Chem.* **1995**, *497*, 91) and probably much higher for β-branched chains, is too high for this to be an important source of stereoerrors.

(5) Reviews: (a) Rappé, A. K.; Skiff, W. M.; Casewit, C. J. *Chem. Rev.* **2000**, *100*, 1435. (b) Angermund, K.; Fink, G.; Jensen, V. R.; Kleinschmidt, R. *Chem. Rev.* **2000**, *100*, 1457.

(6) Busico, V.; Cipullo, R.; Ronca, S. *Macromolecules* **2002**, *35*, 1537.

(7) Busico, V.; Cipullo, R.; Talarico, G.; Caporaso, L. *Macromolecules* **1998**, *31*, 2387.

(8) Busico, V.; Cipullo, R.; Talarico, G.; Segre, A. L.; Caporaso, L. *Macromolecules* **1998**, *31*, 8720.

(9) (a) Ahlrichs, R.; Bär, M.; Baron, H.-P.; Bauernschmitt, R.; Böcker, S.; Ehrig, M.; Eichkorn, K.; Elliott, S.; Furche, F.; Haase, F.; Häser, M.; Hättig, C.; Horn, H.; Huber, C.; Huniar, U.; Kattannek, M.; Köhn, A.; Kölmel, C.; Kollwitz, M.; May, K.; Ochsenfeld, C.; Öhm, H.; Schäfer, A.; Schneider, U.; Treutler, O.; Tsereteli, K.; Unterreiner, B.; Von Arnim, M.; Weigend, F.; Weis, P.; Weiss, H. Turbomole Version 5, January 2002. Theoretical Chemistry Group, University of Karlsruhe, Karlsruhe, Germany. (b) Treutler, O.; Ahlrichs, R. *J. Chem. Phys.* **1995**, *102*, 346.

(10) (a) PQS version 2.4, 2001, Parallel Quantum Solutions, Fayetteville, AK (the Baker optimizer is available separately from PQS upon request). (b) Baker, J. *J. Comput. Chem.* **1986**, *7*, 385.

(11) (a) Lee, C.; Yang, W.; Parr, R. G. *Phys. Rev. B* **1988**, *37*, 785. (b) Becke, A. D. *J. Chem. Phys.* **1993**, *98*, 1372. (c) Becke, A. D. *J. Chem. Phys.* **1993**, *98*, 5648. (d) All calculations were performed using the Turbomole functional "b3-lyp", which is not identical to the Gaussian "B3LYP" functional.

(12) Chan, M. S. W.; Vanka, K.; Pye, C. C.; Ziegler, T. *Organometallics* **1999**, *18*, 4624.

(13) (a) Cossee, P. *J. Catal.* **1964**, *3*, 80. (b) Arlman, E. G.; Cossee, P. *J. Catal.* **1964**, *3*, 99. (c) Grubbs, R. H.; Coates, G. W. *Acc. Chem. Res.* **1996**, *29*, 85. (d) Brintzinger, H. H.; Fischer, D.; Mülhaupt, R.; Rieger, B.; Waymouth, R. M. *Angew. Chem., Int. Ed. Engl.* **1995**, *34*, 1143.

(14) (a) Cavallo, L.; Guerra, G.; Vacatello, M.; Corradini, P. *Macromolecules* **1991**, *24*, 1784. (b) Corradini, P.; Guerra, G.; Cavallo, L.; Moscardi, G.; Vacatello, M. In *Ziegler Catalysts*; Fink, G., Mülhaupt, R., Brintzinger, H. H., Eds.; Springer-Verlag: Berlin, 1995; p 237.

(15) T. Yoshida, N.; Koga, K.; Morokuma *Organometallics* **1996**, *15*, 766. See also ref 16.

(16) L. Castonguay, A.; Rappé, A. K. *J. Am. Chem. Soc.* **1992**, *114*, 5832.
(17) Moscardi, G.; Resconi, L.; Cavallo, L. *Organometallics* **2001**, *20*, 1918.
(18) Reference 4, Figure 16.
(19) Busico, V.; Cipullo, R.; Cutillo, F.; Vacatello, M.; Van Axel Castelli, V. Manuscript in preparation.
(20) Guerra, G.; Cavallo, L.; Moscardi, G.; Vacatello, M.; Corradini, P. *Macromolecules* **1996**, *29*, 4834.
(21) Bierwagen, E. P.; Bercaw, J. E.; Goddard, W. A., III. *J. Am. Chem. Soc.* **1994**, *116*, 1481.
(22) Graf, M.; Jensen, V. R.; Thiel, W. Poster abstract from First Blue-Sky Conference on Catalytic Olefin Polymerization, Sorrento, Italy, 2002.
(23) Guerra, G.; Longo, P.; Cavallo, L.; Corradini, P.; Resconi, L. *J. Am. Chem. Soc.* **1997**, *119*, 4394.
(24) Busico, V.; Cipullo, R.; Segre, A. L. *Macromol. Chem. Phys.* **2002**, *203*, 1403 and references therein.
(25) Arndt, M.; Kaminsky, W.; Schauwienhold, A. M.; Weingarten, U. *Macromol. Chem. Phys.* **1998**, *199*, 1135.

MA034990V